ResearchGate

See discussions, stats, and author profiles for this publication at: https://www.researchgate.net/publication/260380550

Impact of Physical Properties on Ozone Removal by Several Porous Materials

ARTICLE *in* ENVIRONMENTAL SCIENCE & TECHNOLOGY · FEBRUARY 2014

Impact Factor: 5.33 · DOI: 10.1021/es4051956 · Source: PubMed

CITATIONS
4

READS
31

3 AUTHORS, INCLUDING:

Elliott Gall
Nanyang Technological University
25 PUBLICATIONS **114** CITATIONS

SEE PROFILE

Available from: Elliott Gall
Retrieved on: 03 February 2016

Environmental Science & Technology

Article

pubs.acs.org/est

Impact of Physical Properties on Ozone Removal by Several Porous Materials

Elliott T. Gall,[†] Richard L. Corsi,[‡] and Jeffrey A. Siegel*[,§]

[†]Nanyang Technological University and Berkeley Education Alliance for Research in Singapore, Singapore 639798

[‡]The University of Texas at Austin, Austin, Texas 78712, United States

[§]The University of Toronto, Toronto, Ontario M5S 1A4, Canada

Supporting Information

ABSTRACT: Models of reactive uptake of ozone in indoor environments generally describe materials through aerial (horizontal) projections of surface area, a potentially limiting assumption for porous materials. We investigated the effect of changing porosity/pore size, material thickness, and chamber fluid mechanic conditions on the reactive uptake of ozone to five materials: two cellulose filter papers, two cementitious materials, and an activated carbon cloth. Results include (1) material porosity and pore size distributions, (2) effective diffusion coefficients for ozone in materials, and (3) material−ozone deposition velocities and reaction probabilities. At small length scales (0.02−0.16 cm) increasing thickness caused increases in estimated reaction probabilities from 1×10^{-6} to 5×10^{-6} for one type of filter paper and from 1×10^{-6} to 1×10^{-5} for a second type of filter paper, an effect not observed for materials tested at larger thicknesses. For high porosity materials, increasing chamber transport-limited deposition velocities resulted in increases in reaction probabilities by factors of 1.4−2.0. The impact of physical properties and transport effects on values of the Thiele modulus, ranging across all materials from 0.03 to 13, is discussed in terms of the challenges in estimating reaction probabilities to porous materials in scenarios relevant to indoor environments.

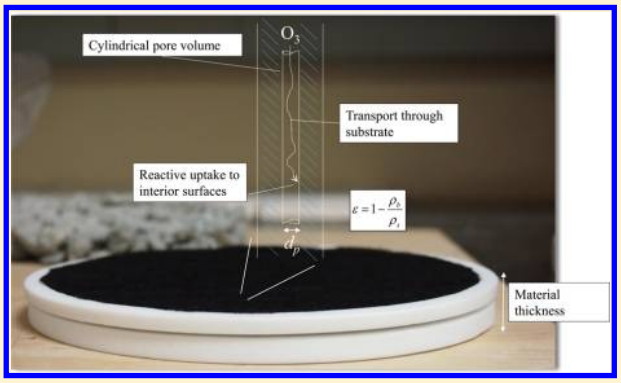

INTRODUCTION

Tropospheric ozone is a regulated air pollutant due to adverse effects on human health including cardiovascular effects, asthma symptoms, and increases in daily mortality.[1−7] Indoor concentrations of ozone are generally lower than outdoor concentrations, largely as a result of reactions with indoor surfaces. However, indoor environments may contribute substantially to human intake of ozone. Weschler[8] estimates 25−60% of total ozone intake occurs indoors, an outcome of Americans spending 87% of their time indoors.[9] A recent investigation demonstrated the importance of indoor ozone in health assessments; explicitly incorporating indoor exposures to ozone explained part of the variability in published mortality coefficients in U.S. cities associated with short-term ozone exposure.[10] Ozone is also highly reactive, and heterogeneous indoor ozone chemistry has important implications for human exposure to irritating or harmful ozone reaction products present indoors.[11] Researchers have broadly characterized indoor ozone−material interactions, ranging from unused materials,[12−15] materials taken from field environments,[16] and experiments in the field.[17] Ozone reactions with indoor surfaces can yield a wide variety of compounds including carbonyls, free radicals, and secondary organic aerosols.[18−21] To address indoor ozone while simultaneously preventing the production of harmful reaction products, there is interest in identifying and using reactive materials with benign ozone reaction products for interior building surface areas and envelopes.[16,22−27]

Material−ozone interactions are generally characterized by determining a first-order loss rate, L (μg s^{-1}) and calculating the deposition velocity (eq 1):

$$v_d = \frac{L}{CA} \tag{1}$$

where v_d is the steady-state ozone deposition velocity (cm s^{-1}), C is the bulk ozone concentration (μg cm^{-3}), and A is the projected area of the material (cm^2). Resistance uptake theory[28,29] can be applied to describe the deposition velocity in terms of a transport limited deposition velocity, v_t (cm s^{-1}), and a reaction probability, γ (-), defined as the fraction of collisions that result in a reaction, as shown in eq 2:

$$\frac{1}{v_d} = \frac{1}{v_t} + \frac{4}{\langle v \rangle \gamma} \tag{2}$$

where $\langle v \rangle$ is the Boltzmann velocity (cm s^{-1}).

Received: November 21, 2013
Revised: February 13, 2014
Accepted: February 25, 2014
Published: February 25, 2014

 © 2014 American Chemical Society dx.doi.org/10.1021/es4051956 | Environ. Sci. Technol. 2014, 48, 3682−3690

Generally, ozone surface reaction rates are estimated following the approach outlined in eqs 1 and 2, as summarized and critiqued previously by Nazaroff et al.[30] While this approach can separate surface reaction phenomena from bulk fluid mechanics, there are several important limitations: (1) deposition velocity calculations require an area, usually a projected area, that does not take into account the complexity of porous surfaces, and (2) transport into and reactions within material substrates are lumped into v_d. For some materials and fluid mechanic conditions, these limitations may prevent identification of phenomena that can affect estimates of ozone removal. For example, Klenø et al.[12] report wide variability in ozone removal to similar building materials, finding ozone deposition velocities to two nylon carpets with latex backing ranging from 1.15 m h^{-1} to 25.2 m h^{-1}. Such variability may stem from phenomena such as material aging and soiling but may also result from differences in physical properties of the material and transport phenomena. For example, diffusion into material pore volumes, e.g., as noted by Reiss et al.,[31] may be implicitly combined into the deposition velocity.

Direct comparisons of the effects of the physical properties are rarely present in the literature. In this paper, we take an experimental approach to investigate material characteristics and transport phenomena and their impact on reactive uptake of ozone. This effort may highlight parameters that have important effects on ozone removal, identifying potential causes of variability when estimating ozone deposition velocities to similar materials. Additionally, such efforts may identify common properties of materials with high ozone removal. This is a first step toward developing new approaches for describing and optimizing ozone reactions with materials.

METHODS AND MATERIALS

Experiments were conducted to explore the impact of material composition, material properties (thickness, porosity, and pore size distribution), and transport phenomena on ozone deposition velocities and reaction probabilities. Five materials were chosen to cover wide ranges of chemical compositions and material properties: two cellulose filter papers (Whatman, GE Healthcare) at varying manufacturer-specified particle retention diameter, 20−25 μm (WF14) and 2.5 μm (WF15); two cementitious materials, a pervious pavement (PP) and a Portland cement concrete (PCC); and an activated carbon cloth (ACC) consisting of 50% activated carbon by mass impregnated on a polyester backing (P/N CO150, Gremarco Industries). Test materials were chosen to compare estimates of reactive uptake of ozone resulting from differences in thickness, porosity/pore size distribution, and chamber fluid mechanics across materials. Filter papers (WF14 and WF15) had identical chemical composition, variable thickness by stacking sheets, and variable porosity/pore size through manufacturer-specified differences in particle retention. Pervious pavement and Portland cement concrete were fabricated with similar raw materials to custom thicknesses while variations in aggregate and sand loadings resulted in variable porosity/pore size. Portland cement concrete also provided a basis of comparison for mercury intrusion porosimeter results.[32] Finally, activated carbon cloth was included due to its anticipated high internal surface area and high effective diffusion coefficient, as well as an opportunity to compare v_d and γ results with previous investigations using this material.[16,33] Material masses, thicknesses, and fabrication methods of the cementitious materials are summarized in the Supporting Information.

Characterization of Physical Properties of Materials. Quantitative descriptions of material pores were made with mercury intrusion porosimetry (MIP, AutoPore III Model 9410, Micromeritics). This allowed determination of material pore size distribution, internal pore area, and porosity by applying stepwise increases in pressure to a penetrometer containing a material sample and elemental mercury. The applied pressure and intruded mercury volume was converted to a pore size distribution (PSD) via the Washburn equation, described in greater detail by Blondeau et al.[32] By assuming a cylindrical pore volume, the PSD was used to determine the internal pore area of a sample. Material porosity, ε (-), was determined by eq 3:

$$\varepsilon = 1 - \frac{\rho_b}{\rho_s} \tag{3}$$

where ρ_b is the bulk density (g mL^{-1}) and ρ_s is the skeletal density (g mL^{-1}), both determined by the MIP.

Instrument limitations affected several estimates of material properties. Filling pressures were set to the lowest possible value, 6.9 kPa, to capture large pores. Maximum pressures were 90 MPa for the filter papers (WF14 and WF15) and 414 MPa for the cementitious materials and activated carbon cloth. A full description of MIP settings is provided in the Supporting Information. Two materials, PP and ACC, contained measurable pores larger than the diameter corresponding to the 6.9 kPa filling pressure (approximately 300 μm) due to the connections of mortar covered aggregate and woven polyester substrate, respectively. Therefore, new values of ρ_b were determined by measuring the dimensions and mass of PP and ACC samples with a vernier caliper (Model 6420, Central Tool Company) and a laboratory balance (VA-16000, Acculab), respectively. Corrections were also made to the MIP-determined median pore diameter by volume for PP and ACC. Fifty measurements of visible pores in each material were made with a vernier caliper and the median reported in place of the MIP-determined value.

Characterization of Diffusion Phenomena. Effective diffusion coefficients for ozone (D_e) were measured to estimate the rate of diffusion of ozone through void spaces in each material. Effective diffusion coefficients were determined in triplicate with an electro-polished, dual-chamber apparatus (Figure S1 in Supporting Information), where test materials were sealed in a flange that separated the chamber into two equal volumes. The conceptual approach followed that of researchers who have measured internal diffusion of VOCs through building materials;[34,35] however, we monitored the migration of sulfur hexafluoride (SF_6) across materials. The SF_6 tracer has been used previously in effective diffusion coefficient experiments[36] and was assumed nonreactive and nonsorptive with chamber and material surfaces.[37,38] Sulfur hexafluoride was injected into the top chamber and monitored by sampling 30-mL volumes of air from the top and bottom chamber at a known time interval using a syringe. Samples were immediately analyzed following extraction using gas chromatography with electron capture detection (Autotrac, Lagus Applied Technology). During extraction of samples, 30-mL volumes of makeup air were supplied to the chamber to minimize the pressure differential across the material. A mass-balance model (see Supporting Information) describing the rate of change of SF_6

dx.doi.org/10.1021/es4051956 | Environ. Sci. Technol. 2014, 48, 3682−3690

concentration across the two volumes separated by the material allowed estimation of D_e for SF_6, accounting for material thicknesses, projected material area, and dilution of chamber SF_6 concentration from makeup air.

Values of D_e for SF_6 can be related to the D_e for ozone by assuming the ratio of molecular diffusion coefficients for SF_6 and ozone in air is equal to the ratio of effective diffusion coefficients for SF_6 and ozone in material pores,[36] and solving for $D_{e,ozone}$, as described by eq 4:

$$D_{e,ozone} = D_{e,SF_6}\frac{D_{ozone}}{D_{SF_6}} \quad (4)$$

where D refers to the molecular diffusion coefficient ($cm^2\ s^{-1}$) in air, and D_e is the effective diffusion coefficient ($cm^2\ s^{-1}$) in a test material, respectively, of the indicated species (ozone and SF_6). As quality assurance, D_e was determined for paper-backed gypsum wallboard to compare with previously reported values; D_e to gypsum board here was 71% of the value reported by Corsi et al.[36] indicating the procedure reasonably reproduced D_e for a similar material.

The mean diffusion coefficient, D^0 ($cm^2\ s^{-1}$), describes the impact of the pore diameter on diffusion in materials and was determined from the pore size distribution and D. The tortuosity, τ (-), relates the length of a curve to the distance between its ends, and has been proposed as accounting for nonidealities in pore structure.[39] This term was calculated with the porosity, D^0, and D_e. Further details outlining the process of calculating both D^0 and τ are provided by Blondeau et al.[32]

Ozone Experiments. Ozone deposition velocities and reaction probabilities were determined in triplicate with the apparatus shown in Figure S2 of the Supporting Information, with analysis of steady-state ozone concentration data described elsewhere.[15] Materials were covered with material- and thickness-specific poly(tetrafluoroethylene) (PTFE) barriers and individually placed in an electro-polished stainless steel chamber (CTH-24, Eagle Stainless). Lab air entering the chamber was cleaned with activated carbon and dehumidified with drierite (Drierite Company, Xenia, OH, USA), and relative humidity (RH) was then controlled by splitting air flow into two streams modulated by rotameters (PMR-010797, Gilmont), one of which passed through an impinger (Model 31760-300, Pyrex) filled with distilled water. Temperature and RH were recorded (Model U12, Onset) every 5 min in Dilution Chamber 2. Tests were conducted at 23.4 ± 0.3 °C and 51 ± 2% RH (mean ± standard deviation) across all experiments.

Ozone was generated from pure oxygen (99% purity, Airgas) using a corona-based ozone generator (Model OL80WT, Yanco Industries). Ozone concentrations in Dilution Chamber 2 and the reaction chamber were measured with an ozone monitor (Model 205, 2B Technologies), calibrated every 2 weeks (Model 306, 2B Technologies). Ozone concentrations entering the reaction chamber were 105 ± 6 ppb (mean ± standard deviation) across all experiments. Flow rates through the reaction chamber resulted in an air exchange rate of 11.7 ± 0.1 h^{-1} (mean ± standard deviation) across all experiments, held constant by mass flow controllers (FMA 5400, Omega) and verified by a bubble flow meter (Gilibrator 2, Sensidyne LP) . A minimum of one background experiment, consisting of the chamber and a PTFE material holder, was run each day experiments were conducted. The average of background loss rates of ozone with the chamber and specific PTFE barrier was then subtracted from the appropriate loss rate with a material present. Background v_d were, on average, less than 0.003 cm s^{-1}. Materials were tested under two fluid mechanic conditions, one with the chamber inlet directly impinging on the material (high v_t, average across all experiments = 1.1 cm s^{-1}) and a second with the inlet port altered to direct flow toward chamber walls (low v_t, average across all experiments = 0.17 cm s^{-1}). Values of v_t were determined for each material type and at each fluid mechanic condition by coating material surfaces with a solution of 100 g of potassium iodide (≥99% purity, Sigma Aldrich) dissolved in 125 mL of distilled water. Reaction probabilities were calculated using the appropriate v_t, v_d, and literature values for $\langle v\rangle$ (360 m s^{-1} for O_3 at 20 °C) in eq 2.

Internal effectiveness factors, η (-), were determined to relate observed rates of material−ozone reactions to the rate of reaction that would be present if no diffusional limitations on transport through materials existed. This relationship, outlined in detail by Hill,[40] is described by eq 5:

$$\eta = \frac{\tanh\phi}{\phi} \quad (5)$$

where ϕ is the Thiele modulus (-), which relates the rate of reaction to the rate of diffusion through the material substrate and is described by eq 6 for a first-order reaction occurring in a material with straight cylindrical pores:[40]

$$\phi = \left(\frac{4k''z^2}{d_{p,A}D_e}\right)^{0.5} \quad (6)$$

where k'' is the surface area-normalized reaction rate constant (cm s^{-1}), Δz is the length of a pore (cm), assumed in this analysis to be the thickness of the material, $d_{p,A}$ (cm) is the area-weighted average pore diameter, and other terms are as defined previously.

To approximate a reaction rate constant independent of bulk fluid mechanics, estimates of reaction probability determined with eq 2 were used to describe k'' described by eq 7:

$$k'' = \frac{\gamma\langle v\rangle\frac{A}{V}}{4S_a\rho_b} \quad (7)$$

where S_a is the pore area per unit mass ($cm^2\ g^{-1}$), p_b is the bulk density of the material (g cm^{-3}), and all other terms are as defined previously.

RESULTS AND DISCUSSION

Physical properties determined in this investigation (Section 3.1) affect material transport phenomena (Section 3.2), and both physical properties and transport phenomena affect reactive uptake of ozone to materials (Section 3.3). This investigation identifies and quantifies differences in physical properties and material transport phenomena that are then used to estimate dimensionless parameters that explain observed impacts on ozone deposition velocities and reaction probabilities. Comparisons are made across the five materials, to the same material at varying thickness, and to similar materials with varying porosity and pore size distribution at two fluid mechanic conditions.

Physical Properties. Materials were selected with variable physical properties to inform qualitative explanations of differences in transport phenomena and reactive uptake of ozone to materials. Differences in porosity and pore size

dx.doi.org/10.1021/es4051956 | Environ. Sci. Technol. 2014, 48, 3682−3690

Table 1. Summary of Physical Properties of Materials

material	porosity, ε (-)	median pore diameter (volume), $d_{p,V}$ (μm)	median pore diameter (area), $d_{p,A}$ (μm)	pore area, S_a (m^2 g^{-1})
20−25 μm filter paper, WF14	0.77	13	0.51	14
2.5 μm filter paper, WF15	0.78	15	0.39	19
pervious pavement, PP	0.67[a]	2700[b]	0.044	2.5
Portland cement concrete, PCC	0.26	0.19	0.054	13
activated carbon sheet, ACC	0.97[a]	500[b]	0.036	160

[a]Porosity is corrected for pervious pavement and activated carbon cloth by substituting a corrected material bulk density into eq 4 (see Section 2.1). [b]Values for median pore diameter by volume for these materials are corrected according to the methodology described in Section 2.1.

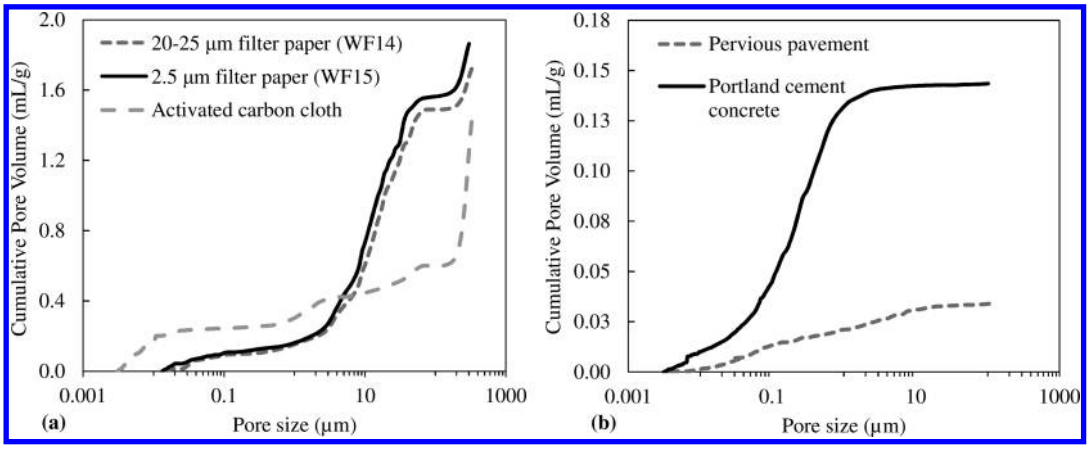

Figure 1. Cumulative pore size distributions determined by mercury intrusion porosimetry. Higher porosity materials are grouped in panel a, while lower porosity materials are grouped in panel b. Material void volumes corresponding with pore diameters greater than the filling pressure of the mercury intrusion porosimeter (approximately 300 μm or a filling pressure of 6.9 kPa) are not accounted for in these distributions.

Table 2. Average Effective Diffusion Coefficients of Ozone through Materials

material	effective diffusion coefficient, D_e (cm^2 s^{-1})[a]	mean diffusion coefficient, D^0 (cm^2 s^{-1})	tortuosity, τ (-)
20−25 μm filter paper, WF14	0.033 ± 0.003	0.1497	3.2
2.5 μm filter paper, WF15	0.024 ± 0.001	0.1476	5.4
pervious pavement, PP	0.021 ± 0.004	0.1345	4.5
Portland cement concrete, PCC	0.0024 ± 0.0001	0.1359	14
activated carbon sheet, ACC	0.12 ± 0.01	0.1337	1.1

[a]Uncertainty in effective diffusion coefficients is the standard deviation across triplicate experiments.

distribution (PSD) were expected for the two types of filter paper studied, given the manufacturer-specified difference in particle retention diameter (WF14 at 20−25 μm versus WF15 at 2.5 μm). However, these materials have similar porosities and pore areas (Table 1 and Figure 1a). It is possible that the experimental uncertainty associated with mercury intrusion porosimetry (MIP) was unable to differentiate pore diameters in the supermicrometer range, where stepwise pressure increases resulted in large increases in intruded mercury volumes in the 1−30 μm range. Such increases may obscure small differences in pore diameter−intrusion relationships. The data in Table 1 and Figure 1 derive from single MIP runs for each material, and therefore experimental error could not be reliably quantified. However, previous work estimates experimental error in porosity measurements determined with MIP to range from 4% to 6%.[41,42]

In contrast to the filter papers, there were substantial differences in experimentally determined PSDs between pervious pavement (PP) and Portland cement concrete (PCC). While the components of each material were similar (aggregate, cement, water, and in the case of PCC, sand), because the PP mixture contained no sand, the final product was a network of mortar-covered aggregate. This leads to a larger pore diameter and greater porosity for PP, while the presence of sand resulted in a smaller pore diameter and lower porosity for PCC.

In the case of activated carbon cloth (ACC), an abrupt jump in volume in the pore diameter range of 200−300 μm is exhibited in Figure 1a. This is due to the presence of large pores resulting from the woven polyester backing that provides structural support to the sheet. In addition, ACC also has a high volume of pores in the 0.003−0.3 μm pore diameter range. This is the cause for the substantially higher pore area for ACC than other materials, as reported in Table 1.

Where available, comparisons of physical material properties with values determined in the literature yield mixed results. The ACC analyzed here has approximately half the internal surface area of an activated carbon cloth measured by Grøntoft.[13] Porosity of the PCC shown in Table 1 is similar to the value of 0.299 for aerated concrete analyzed with MIP by Blondeau et al.,[32] while the pore area measured here is an order of magnitude higher.

Diffusion through Materials. Experiments measuring diffusion through materials were conducted under similar environmental conditions. Therefore, differences in the effective diffusion coefficient (D_e) arise from variations in

dx.doi.org/10.1021/es4051956 | Environ. Sci. Technol. 2014, 48, 3682−3690

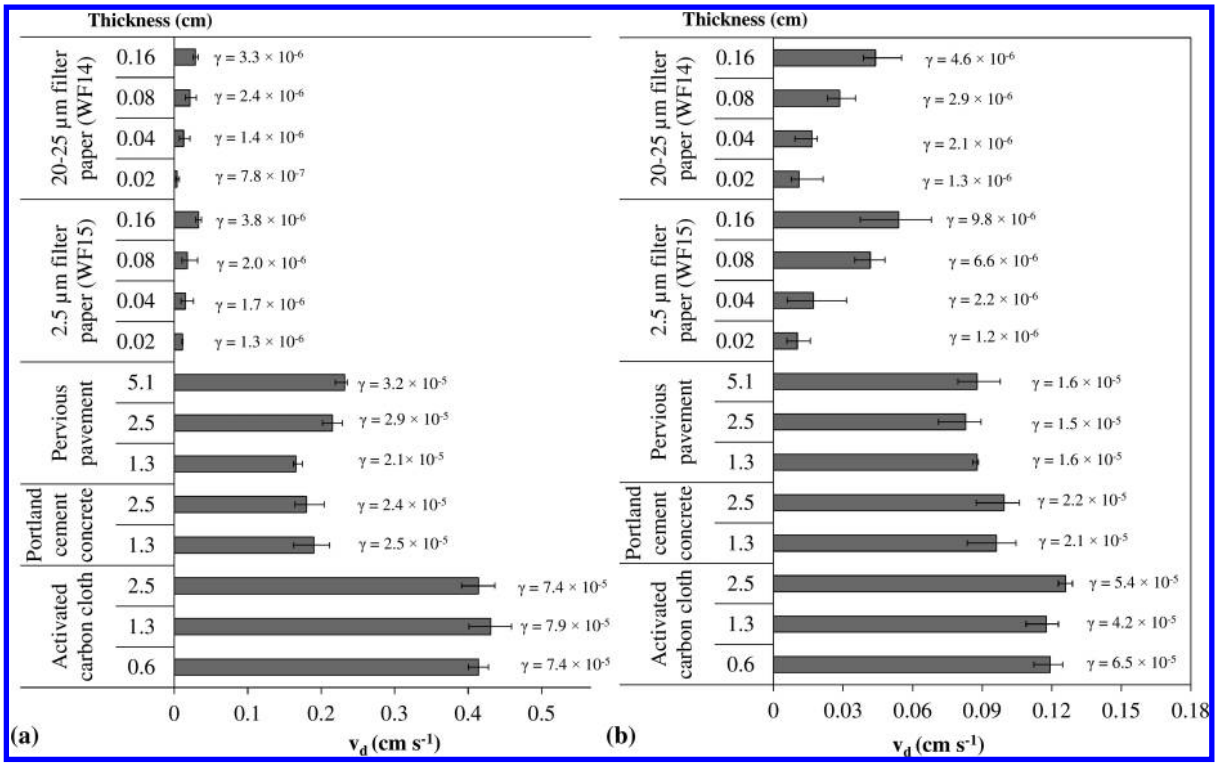

Figure 2. Average ozone deposition velocities to materials under (a) high v_t and (b) low v_t. Material thickness (cm) is adjacent to the material name. Error bars reflect the range associated with triplicate experiments. Material−ozone reaction probabilities are shown at the top of each bar, determined with eq 2 using average values of v_d across triplicate experiments, and v_t and $\langle v \rangle$ from independent experiments and the literature, respectively.

material structures, where pore size, porosity, and tortuosity play roles in determining the rate of diffusion of a compound through materials. Effective diffusion coefficients for ozone are reported for the five materials in Table 2, with accompanying estimates of mean diffusion coefficients (D^0) and tortuosity (τ). The D_e of the WF15 filter paper sample was 73% of the value of the WF14 sample, an unanticipated finding given that the MIP analyses revealed similar material properties. However, a small increase in nanometer-scale pores in the WF15 sample resulted in a slightly smaller D^0, also reflected in the reduced area-weighted median pore diameter for the WF15 sample. Differences in D_e and D^0 are propagated to the determination of the material tortuosity, implying that reductions in D_e from WF14 to WF15 are due to the more tortuous paths present in WF15.

In contrast to the filter papers, estimates of D_e for the two cementitious materials were markedly different. Pervious pavement (PP) had a D_e 8.5 times larger than that of the Portland cement concrete (PCC). The mortar-covered aggregates that composed the PP had lower porosity and smaller pore diameters than PCC, but the higher D_e for PP is the result of large openings between the connected aggregate in the assembled material. The PCC had the lowest D_e of the materials studied, an expected result given the small volume-weighted median pore diameter and low porosity of this material. Figure 1 shows the presence of substantial pore volume (34%) being contributed from pore diameters less than 0.1 μm, where wall interactions begin to affect diffusion mechanisms in the pore. This, coupled with the lower overall porosity and high tortuosity, contributes to a reduced D_e for PCC.

The ACC had a D_e of 0.12 cm^2 s^{-1}, near the molecular diffusion coefficient of ozone in air at 25 °C of 0.18 cm^2 s^{-1} reported by Massman.[43] This is due to the presence of substantial pore volumes with supermicrometer diameters that, combined with a very large porosity, result in a D_e that approaches D. Figure 1 and Table 1 also show that ACC has a large internal surface area, a result of the presence of pore diameters in the nanometer range. It is possible that the large pore diameters in ACC may have increased the determined D_e by transporting SF_6 across the material via advective, and not diffusive, processes. However, repeatable values of D_e for ACC slightly below D provides evidence that diffusive transport dominated, as even small pressure drops induced over ACC would result in rapid advection across the material, causing D_e to exceed D.

Ozone Reactions with Materials. Differences in material composition and properties, transport phenomena, and chamber fluid mechanics contribute to differences in ozone deposition velocities (v_d) and reaction probabilities (γ). For the five test materials, v_d ranged from 0.021 cm s^{-1} to WF14 filter paper at low v_t to 0.42 cm s^{-1} to activated carbon cloth (ACC) at high v_t, summarized in Figure 2. Variability in v_d and γ was observed across thickness conditions for filter papers and pervious pavement, discussed in greater detail in Section 3.4.1. Variability in v_d and γ was not observed with changes in porosity/pore size of filter papers or cementitious materials, an important finding for the comparison of pervious pavement (PP) and Portland cement concrete (PCC, see Section 3.4.2). Finally, the observed differences in v_d and γ across fluid mechanic conditions for PP and ACC is discussed in Section 3.4.3.

The variability in deposition velocities across material properties and fluid mechanic conditions highlight difficulties in making comparisons with values determined by other researchers. A comparison of v_d with values published in the

dx.doi.org/10.1021/es4051956 | Environ. Sci. Technol. 2014, 48, 3682−3690

Table 3. Estimations of Reaction and Diffusion Phenomena in Test Materials, Shown As the Numerator and Denominator of the Expression for Thiele Modulus, Respectively[a]

			high v_t			low v_t		
	thickness, Δz (cm)	$d_{pA}D_e$ ($cm^3\ s^{-1}$)	$4k''\Delta z^2$ ($cm^3\ s^{-1}$)	Thiele modulus, ϕ (-)	internal effectiveness factor, η (-)	$4k''\Delta z^2$ ($cm^3\ s^{-1}$)	Thiele modulus, ϕ (-)	internal effectiveness factor, η (-)
20–25 μm filter paper, WF14	0.2	1.7×10^{-6}	6.0×10^{-9}	0.060	0.99	2.1×10^{-9}	0.033	0.99
	0.4		6.9×10^{-9}	0.064	0.99	1.3×10^{-8}	0.053	0.99
	0.8		1.6×10^{-8}	0.10	0.99	7.3×10^{-8}	0.09	0.99
	1.6		4.9×10^{-8}	0.17	0.99	4.7×10^{-8}	0.14	0.99
2.5 μm filter paper, WF15	0.2	7.8×10^{-7}	1.4×10^{-9}	0.042	0.99	2.0×10^{-9}	0.043	0.99
	0.4		4.2×10^{-9}	0.074	0.99	1.4×10^{-9}	0.065	0.99
	0.8		1.4×10^{-8}	0.14	0.99	1.7×10^{-7}	0.075	0.99
	1.6		3.1×10^{-8}	0.20	0.98	1.0×10^{-6}	0.12	0.99
pervious pavement, PP	13	9.2×10^{-8}	5.5×10^{-7}	2.4	0.40	7.2×10^{-7}	2.8	0.36
	25		2.1×10^{-6}	4.8	0.21	4.1×10^{-6}	6.7	0.15
	51		8.1×10^{-6}	9.4	0.11	1.6×10^{-6}	13	0.077
Portland cement concrete, PCC	13	1.4×10^{-8}	1.1×10^{-7}	2.8	0.35	1.2×10^{-7}	3.0	0.33
	25		4.5×10^{-7}	5.8	0.17	4.9×10^{-7}	6.0	0.17
activated carbon sheet, ACC	6	4.7×10^{-7}	3.7×10^{-8}	0.28	0.97	6.2×10^{-8}	0.36	0.96
	13		1.5×10^{-7}	0.56	0.91	2.7×10^{-7}	0.76	0.84
	25		6.0×10^{-7}	1.1	0.72	8.2×10^{-7}	1.3	0.66

[a]Values of the Thiele modulus and the internal effectiveness factor are calculated from experimentally determined physical material properties under high and low mass transfer conditions (v_t).

literature is not possible for the specific filter papers used in this study. However, Klenø et al.[12] observed higher values of v_d to office paper at >1.49 cm s^{-1}. Poppendieck et al.[44] determined ozone deposition velocities of 0.06 cm s^{-1} to a stack of 50 sheets of typical office paper at high inlet ozone concentrations (>1000 ppm), a higher value than observed in the 0.16 cm thickness condition (8 sheets of WF14) in this study. Grontoft and Raychaudhuri[45] characterized v_d to coarse and fine concrete, estimating 0.08 and 0.017 cm s^{-1}, respectively, lower than the average value across low and high v_t determined in this work (0.14 cm s^{-1}) determined here for PCC. Ozone deposition velocities to ACC have been characterized more extensively in the literature, with values ranging from 0.069 to 0.22 cm s^{-1}, over three independent investigations,[13,16,33] generally lower but overlapping with the range of values averaged across all thicknesses at low and high v_t determined in this study, i.e., from 0.12 to 0.42 cm s^{-1}, respectively.

Material composition should dictate the likelihood of a reaction given an ozone–material collision, described by the reaction probability, γ. However, in material testing scenarios relevant to indoor environments, transport phenomena and substrate effects may be lumped into v_d and then propagated into estimations of the reaction probability. At high v_t, Figure 2 lists average ozone reaction probabilities for the five materials across all thicknesses that range from 1.3×10^{-6} for WF14 to 7.9×10^{-5} for the activated carbon cloth (ACC). At low v_t, values range from 1.2×10^{-6} for WF14 to 7.9×10^{-5} for ACC. Averaged across all materials, values of reaction probability across fluid mechanic conditions are within ±40%.

Impact of Physical and Transport Properties on Ozone–Material Reactions. The variations in estimations of γ across thickness condition (WF14 and WF15) and v_t condition (PP and ACC) in Figure 2 are evidence of deviations from assumptions of horizontal projections of material surface area and indicate transport and reaction of ozone is occurring in material substrates. Reaction probability to a single material varies by as much as an order of magnitude, e.g., across thickness conditions for WF15 at low v_t. Other researchers have determined v_d with internal surface areas;[13] however, because in the cases of WF14 and WF15 v_d increases with thickness, any single value of surface area with varying material thickness will not result in a constant value of γ. The Thiele modulus (determined from eq 6), shown in Table 3 with corresponding estimates of the internal effectiveness factor (eq 5), relates the rate of reaction to the rate of transport in pore volumes present in materials. These terms combine the impact of physical properties described in Section 3.1, transport phenomena described in Section 3.2, and reaction rates described in Section 3.3 to the relative importance of diffusive and reactive phenomena in material substrates.

Values of the Thiele modulus less than unity indicate that reaction processes are slow relative to diffusion processes and ozone removal is reaction-limited, while values greater than unity indicate reactions are occurring quickly relative to internal diffusion and ozone removal is internal diffusion-limited. Estimations of the Thiele modulus were made for each experimental scenario and ranged from 0.03 for 0.02 cm WF15 at low fluid mechanic conditions to 13 for 2.5 cm PP at low fluid mechanic conditions. These values of Thiele modulus corresponded to a range of internal effectiveness factors from >0.99 to 0.10. This indicates that across the conditions studied, ozone removal to test materials ranged from reaction-limited to internal diffusion-limited; the contribution of physical material properties to the calculation of the ϕ and η are discussed in subsequent sections.

Impact of Thickness. Ozone deposition velocities (v_d) and reaction probabilities (γ), shown in Figure 2, increased with increases in material thickness for the two types of cellulose filter paper (WF14 and WF15) at both high and low v_t and for pervious pavement (PP) at high v_t. On average, the 0.16 cm conditions of WF14 and WF15 had four times higher v_d than the 0.02 cm conditions and five times higher γ. Table 3 shows that WF14 and WF15, under all conditions, have ϕ less 0.2 and η of 0.98 or greater, indicating that these materials are reaction-

dx.doi.org/10.1021/es4051956 | Environ. Sci. Technol. 2014, 48, 3682–3690

limited. The small values of Thiele modulus are a function of small thickness scales (Δz), moderate effective diffusion coefficients (D_e), and slow reaction rate (k'') relative to other test materials. This results in internal area throughout the entire ranges of thicknesses (0.02−0.16 cm) contributing to the determined deposition velocity. Therefore, for materials with low values Thiele modulus (<0.2), resistance-uptake theory as defined in eqs 1 and 2 may not be appropriate for describing interactions between ozone and materials in indoor environments.

Figure 2 also shows increases in v_d and γ for PP with increases in thickness at high v_t. High values of ϕ are determined for this material, shown in Table 3, with low values of η. This implies an internal transport-limited condition that indicates additional thickness should not increase reactions. The large median pore diameter by volume of PP ($d_{p,V}$ = 2700 μm) compared to the median pore diameter by area ($d_{p,A}$ = 0.044 μm) increases the likelihood of advective flow through the material under high v_t conditions. This could contribute to concentration gradients in pore volumes present between connected aggregate, as well as in pore volumes within aggregate characterized by the $d_{p,A}$. These effects would not be captured in the estimation of the Thiele modulus, a one-dimensional representation of internal reaction and diffusion.

Ozone deposition velocities to PCC had no dependence on thickness, which is logical given its high Thiele modulus and low internal effectiveness factor. Activated carbon cloth (ACC) also showed no dependence on thickness at either low or high v_t. This was an unexpected result given the high D_e determined for this material. Additionally, the large pores (>300 μm) in ACC would result in advective flow from a relatively low pressure differential across the material, following logic similar to that discussed for PP. However, high reaction probabilities for ACC, a relatively smaller $d_{p,V}$ compared to that for PP, and a high internal pore area result in η ranging from 0.66 to 0.97 across all conditions, implying that reactions occur more rapidly than diffusive processes can transport ozone throughout the material.

Further investigation of the transport mechanisms through materials under changing bulk fluid mechanic conditions is warranted to better explain the impact of material thickness on ozone removal to materials, especially those with large pore diameters for which advection may play a role. Results for filter papers and pervious pavement show that increasing thickness may only enhance ozone removal for certain materials under specific fluid mechanic and material porosity/pore size conditions. For example, it appears that moderately reactive materials with large pore diameters (e.g., PP) may result in decreased chamber (or room) ozone concentrations at high v_t. At millimeter thickness scales, i.e., WF14 and WF15, D_e on the order of 0.02−0.03 cm^2 s^{-1} appears sufficient to result in transport and reaction in material substrates with lower overall v_d.

Impact of Porosity and Pore Size. Porosity and pore size may affect ozone removal in several important ways. As discussed previously, rates of advective or diffusive transport into materials may be impacted by porosity and pore size. Both of these terms also affect the material pore area, which is proportional to the number of ozone reaction sites. Additionally, because porosity and pore size are more difficult to measure than, for example, material thickness, there is potential for variation in porosity and pore size to contribute to uncertainty in comparisons of estimates of v_d to apparently similar materials.

In this investigation, porosity and pore size had mixed and indirect implications on reported estimates of v_d. No differences in v_d or γ exceeding experimental uncertainty were observed between the filter papers (WF14 and WF15) at either low or high v_t. Due to the similar measured properties (e.g., $d_{p,V}$, ε, D_e) of these two materials it may not have been possible to detect a difference in v_d, if one existed at all. In the case of PP and PCC, similar values for average v_d were noted for each material at each v_t investigated. This stems from offsetting transport and reaction phenomena in the substantially different structure of each material. Values of Thiele modulus determined for these materials were similar, e.g., ranging from 2.4 to 4.5 and 2.8 to 5.7 across 13 to 25 cm thickness for PP and PCC, respectively, at low v_t. This is a result of a trade-off in eq 7, where the larger D_e of PP is offset by a greater pore area in PCC. Therefore, η is reduced for PP due to rapid diffusion but insufficient internal pore area, while η is reduced for PCC because of slow diffusion through the material. This implies reaction probabilities to these two materials should be dissimilar. However, because of similar v_d and a constant value of projected area input to eq 2 for these two materials, γ values for PP and PCC determined in this investigation are similar.

Impact of Fluid Mechanics. Bulk fluid mechanics affect estimates of v_d; however, unlike thickness, porosity, and pore size, fluid mechanic effects can be accounted for through the determination of a transport-limited deposition (eq 2). Increases in v_d at high v_t for all materials were expected and were found for all thicknesses of PP, ACC, and PCC. There were observable differences in v_d for only three of the eight comparisons for Whatman filters. It appears that v_d for thicker materials (ACC, PCC and PP) increased with an increase in v_t, while thinner materials (WF14 and WF15) did so less consistently. This implies that at the length scales of the Whatman filters, the more limiting step for reaction is not diffusion through the concentration boundary layer but the decreased quantity of ozone reaction sites through a smaller thickness of material, supported by estimates of η of >0.99 for WF14 and WF15.

Reaction probabilities across fluid mechanic conditions are most similar for PCC and most dissimilar for PP and ACC. This is reflective of the properties of PCC (a steep PSD with small d_p, low D_e, and low ε) compared to PP and ACC (flatter PSDs with larger d_p, high D_e, and high ε) that make PCC more closely approximate the flat-plate assumption often used when applying resistance-uptake theory. In theory, ϕ and η should be independent of bulk fluid mechanics, with k'' being derived with the reaction probability (eq 7). Estimations of η were most similar across fluid mechanic conditions for similar thickness conditions of WF14, WF15, and PCC, with an average difference across all materials of ±1.3%, and were most dissimilar for PP and ACC, with an average difference of ±14%. The larger differences for PP and ACC likely stem from two-dimensional concentration gradients throughout the materials driven first by advective transport into the gaps between interconnected material (characterized by $d_{p,V}$) followed by diffusion and reaction into small pores present in the material (characterized by $d_{p,A}$).

The variability in reactive uptake of ozone among similar indoor materials observed in this study illustrates challenges and benefits associated with deeper characterization of material properties and effective diffusion coefficients and their

implications for estimations of ozone deposition velocity and reaction probability. The determination of the Thiele modulus is a useful quantitative metric in determining the appropriateness of applying resistance-uptake theory to estimations of ozone removal to material surfaces with varying physical properties. Materials with high Thiele modulus and steeper PSDs (e.g., PCC) appear most well-suited for description with resistance uptake theory. At low values of Thiele modulus, a reaction-limited condition and high internal effectiveness factors result in a relationship between material thickness and γ not captured by resistance-uptake theory. Finally, determinations of v_d and γ for high Thiele modulus materials with flatter PSDs (PP and ACC) may be affected by advective transport into bulk materials under some fluid mechanic conditions. Practically, these considerations inform our understanding of the importance of material properties that may enhance reactive uptake of ozone for specific material/environmental condition combinations. This is an important consideration in indoor environments where an abundance of surfaces (e.g., walls, ceilings) have the potential to be covered with materials with thickness on the order of millimeters.

■ ASSOCIATED CONTENT

Supporting Information

Additional information regarding material fabrication methods, MIP settings, and the analytical approach to determine D_e. This material is available free of charge via the Internet at http://pubs.acs.org.

■ AUTHOR INFORMATION

Corresponding Author

*Tel: (416) 978-7975. Fax: (416) 978-6813. E-mail: jeffrey.siegel@utoronto.ca.

Notes

The authors declare no competing financial interest.

■ ACKNOWLEDGMENTS

Elliott Gall was funded by a U.S. EPA STAR Fellowship (no. FP-91733001-0) and an NSF IGERT grant (no. DGE-0549428). We would like to thank Dr. Brent Stephens, Dr. Neil Crain, and Tania de Souza for assistance with D_e experiments, Glen Butler for assistance with MIP, and Dr. Sarah Taylor Lange for guidance fabricating cementitious materials.

■ REFERENCES

(1) U.S. EPA. *Air Quality Criteria for Ozone and Related Photochemical Oxidants. Volume I of III*; EPA 600/R-05/004aF; U.S. EPA, National Center for Environmental Assessment: Arlington, VA, 2006.

(2) Peel, J. L.; Klein, M.; Flanders, W. D.; Mulholland, J. A.; Freed, G.; Tolbert, P. E. Ambient air pollution and apnea and bradycardia in high-risk infants on home monitors. *Environ. Health Perspect.* **2011**, *119*, 1321−1327.

(3) Devlin, R. B.; Duncan, K. E.; Jardim, M.; Schmitt, M. T.; Rappold, A. G.; Diaz-Sanchez, D. Controlled exposure of healthy young volunteers to ozone causes cardiovascular effects. *Circulation* **2012**, *126*, 104−111.

(4) Romieu, I.; Meneses, F.; Ruiz, S.; Huerta, J.; Sienra, J. J.; White, M.; Etzel, R.; Hernandez, M. Effects of intermittent ozone exposure on peak expiratory flow and respiratory symptoms among asthmatic children in Mexico City. *Arch. Environ. Health* **1997**, *52*, 368−376.

(5) Bell, M. L.; Peng, R. D.; Dominici, F. The exposure-response curve for ozone and risk of mortality and the adequacy of current ozone regulations. *Environ. Health Perspect.* **2006**, *114*, 532−536.

(6) Bell, M. L.; McDermott, A.; Zeger, S. L.; Samet, J. M.; Dominici, F. Ozone and short-term mortality in 95 US urban communities, 1987−2000. *J. Am. Med. Assoc.* **2004**, *292*, 2372−2378.

(7) Levy, J. I.; Chemerynski, S. M.; Sarnat, J. A. Ozone exposure and mortality: an empiric bayes metaregression analysis. *Epidemiology* **2005**, *16*, 458−468.

(8) Weschler, C. J. Ozone's impact on public health: contributions from indoor exposures to ozone and products of ozone-initiated chemistry. *Environ. Health Perspect.* **2006**, *114*, 1489−1496.

(9) Klepeis, N. E.; Nelson, W.; Ott, W. R.; Robinson, J. P.; Tsang, A. M.; Switzer, P.; Behar, J. V.; Hern, S. C.; Engelman, W. H. The National Human Activity Pattern Survey (NHAPS): a resource for assessing exposure to environmental pollutants. *J. Exposure Sci. Environ. Epidemiol.* **2001**, *11*, 231−252.

(10) Chen, C.; Zhao, B.; Weschler, C. J. Assessing the influence of indoor exposure to "outdoor ozone" on the relationship between ozone and short-term mortality in U.S. communities. *Environ. Health Perspect.* **2012**, *120*, 235−240.

(11) Wolkoff, P.; Larsen, S. T.; Hammer, M.; Kofoed-Sørensen, V.; Clausen, P. A.; Nielsen, G. D. Human reference values for acute airway effects of five common ozone-initiated terpene reaction products in indoor air. *Toxicol. Lett.* **2013**, *216*, 54−64.

(12) Klenø, J. G.; Clausen, P. A.; Weschler, C. J.; Wolkoff, P. Determination of ozone removal rates by selected building products using the FLEC emission cell. *Environ. Sci. Technol.* **2001**, *35*, 2548−2553.

(13) Grøntoft, T. Dry deposition of ozone on building materials. Chamber measurements and modelling of the time-dependent deposition. *Atmos. Environ.* **2002**, *36*, 5661−5670.

(14) Nicolas, M.; Ramalho, O.; Maupetit, F. Reactions between ozone and building products: Impact on primary and secondary emissions. *Atmos. Environ.* **2007**, *41*, 3129−3138.

(15) Lamble, S. P.; Corsi, R. L.; Morrison, G. C. Ozone deposition velocities, reaction probabilities and product yields for green building materials. *Atmos. Environ.* **2011**, *45*, 6965−6972.

(16) Cros, C. J.; Morrison, G. C.; Siegel, J. A.; Corsi, R. L. Long-term performance of passive materials for removal of ozone from indoor air. *Indoor Air* **2012**, *22*, 43−53.

(17) Wang, H.; Morrison, G. C. Ozone-initiated secondary emission rates of aldehydes from indoor surfaces in four homes. *Environ. Sci. Technol.* **2006**, *40*, 5263−5268.

(18) Weschler, C. J.; Hodgson, A. T.; Wooley, J. D. Indoor chemistry: ozone, volatile organic compounds, and carpets. *Environ. Sci. Technol.* **1992**, *26*, 2371−2377.

(19) Weschler, C. J. Ozone in indoor environments: Concentration and chemistry. *Indoor Air* **2000**, *10*, 269−288.

(20) Springs, M.; Wells, J. R.; Morrison, G. C. Reaction rates of ozone and terpenes adsorbed to model indoor surfaces. *Indoor Air* **2011**, *21*, 319−327.

(21) Waring, M. S.; Siegel, J. A. Indoor secondary organic aerosol formation initiated from reactions between ozone and surface-sorbed D-limonene. *Environ. Sci. Technol.* **2013**, *47*, 6341−6348.

(22) Yu, J.-W.; Neretnieks, I. The effect of a passive adsorption sheet on reducing organic pollutants in indoor air. *Indoor Air* **1993**, *3*, 12−19.

(23) Morrison, G. C.; Nazaroff, W. W. The rate of ozone uptake on carpets: Experimental studies. *Environ. Sci. Technol.* **2000**, *34*, 4963−4968.

(24) Gall, E. T.; Corsi, R. L.; Siegel, J. A. Barriers and opportunities for passive removal of indoor ozone. *Atmos. Environ.* **2011**, *45*, 3338−3341.

(25) Darling, E.; Cros, C.; Wargocki, P.; Kolarik, J.; Morrison, G. C.; Corsi, R. L. Impacts of a clay plaster on indoor air quality assessed using chemical and sensory measurements. *Build. Environ.* **2012**, *57*, 370−376.

(26) Stephens, B.; Gall, E. T.; Siegel, J. A. Measuring the penetration of ambient ozone into residential buildings. *Environ. Sci. Technol.* **2012**, *46*, 929−936.

(27) Taylor-Lange, S. C.; Juenger, M. C. G.; Siegel, J. A. Impact of cement renders on airborne ozone and carbon dioxide concentrations. *Atmos. Environ.* **2013**, *70*, 263−266.
(28) Cano-Ruiz, J. A.; Kong, D.; Balas, R. B.; Nazaroff, W. W. Removal of reactive gases at indoor surfaces: Combining mass transport and surface kinetics. *Atmos. Environ.* **1993**, *27*, 2039−2050.
(29) Finlayson-Pitts, B. J.; Pitts, J. *Chemistry of the Upper and Lower Atmosphere: Theory, Experiments, and Applications*; Academic Press: New York, 1999.
(30) Nazaroff, W. W.; Gadgil, A. J.; Weschler, C. J. *Critique of the Use of Deposition Velocity in Modeling Indoor Air Quality*; ASTM International: West Conshohocken, PA, 1993; pp 81−103.
(31) Reiss, R.; Ryan, P. B.; Koutrakis, P. Modeling ozone deposition onto indoor residential surfaces. *Environ. Sci. Technol.* **1994**, *28*, 504−513.
(32) Blondeau, P.; Tiffonnet, A. L.; Damian, A.; Amiri, O.; Molina, J. L. Assessment of contaminant diffusivities in building materials from porosimetry tests. *Indoor Air* **2003**, *13*, 310−318.
(33) Kunkel, D. A.; Gall, E. T.; Siegel, J. A.; Novoselac, A.; Morrison, G. C.; Corsi, R. L. Passive reduction of human exposure to indoor ozone. *Build. Environ.* **2010**, *45*, 445−452.
(34) Little, J. C.; Hodgson, A. T.; Gadgil, A. J. Modeling emissions of volatile organic compounds from new carpets. *Atmos. Environ.* **1994**, *28*, 227−234.
(35) Bodalal, A.; Zhang, J. S.; Plett, E. G. A method for measuring internal diffusion and equilibrium partition coefficients of volatile organic compounds for building materials. *Build. Environ.* **2000**, *35*, 101−110.
(36) Corsi, R. L.; Crain, N.; Fardal, J.; Little, J.; Xu, Y. *Determination of Sorption Parameters for 36 VOC/Material Combinations Final Report*; EPA 600/R-07/035-R1; U.S. Environmental Protection Agency: Washington, DC, 2007.
(37) Howard-Reed, C.; Wallace, L. A.; Ott, W. R. The effect of opening windows on air change rates in two homes. *J. Air Waste Manag. Assoc.* **2002**, *52*, 147−159.
(38) Ferro, A. R.; Klepeis, N. E.; Ott, W. R.; Nazaroff, W. W.; Hildemann, L. M.; Switzer, P. Effect of interior door position on room-to-room differences in residential pollutant concentrations after short-term releases. *Atmos. Environ.* **2009**, *43*, 706−714.
(39) Woods, J.; Pellegrino, J.; Burch, J. Generalized guidance for considering pore-size distribution in membrane distillation. *J. Membr. Sci.* **2011**, *368*, 124−133.
(40) Hill, C. G. *An Introduction to Chemical Engineering Kinetics & Reactor Design*; Wiley: New York, 1977.
(41) Hearn, N.; Hooton, R. D. Sample mass and dimension effects on mercury intrusion porosimetry results. *Cem. Concr. Res.* **1992**, *22*, 970−980.
(42) Cook, R. A.; Hover, K. C. Mercury porosimetry of hardened cement pastes. *Cem. Concr. Res.* **1999**, *29*, 933−943.
(43) Massman, W. J. A review of the molecular diffusivities of H_2O, CO_2, CH_4, CO, O_3, SO_2, NH_3, N_2O, NO, and NO_2 in air, O_2 and N_2 near STP. *Atmos. Environ.* **1998**, *32*, 1111−1127.
(44) Poppendieck, D.; Hubbard, H.; Ward, M.; Weschler, C.; Corsi, R. L. Ozone reactions with indoor materials during building disinfection. *Atmos. Environ.* **2007**, *41*, 3166−3176.
(45) Grøntoft, T.; Raychaudhuri, M. R. Compilation of tables of surface deposition velocities for O_3, NO_2 and SO_2 to a range of indoor surfaces. *Atmos. Environ.* **2004**, *38*, 533−544.